

# **Role Of Magnetic Resonance Imaging In Diagnosis And Staging Of Prostatic Cancer**

**Essay**

*Submitted for partial fulfillment of Master Degree  
In Radiodiagnosis*

*By*

**Engie El-Sayed Mohamed Ibrahim El-Gohary**  
*M.B., B.Ch.*

*Under The Supervision Of*

**Prof. Dr.Sahar Mohamed El-Feky**

*Professor of Radiodiagnosis  
Faculty of Medicine, Ain Shams University.*

**Dr.Noha Mohamed Othman**

*Lecturer of Radiodiagnosis  
Faculty of Medicine, Ain Shams University.*

**Faculty of Medicine,  
Ain Shams University  
2012**

# دور التصوير بالرنين المغناطيسي في تشخيص وتحديد مراحل سرطان البروستاتا

دراسة مقدمة من الطيبة

انجي السيد محمد ابراهيم الجوهري  
بكالوريوس الطب والجراحة

توطئة للحصول على درجة الماجستير في الأشعة التشخيصية

تحت إشراف

الأستاذة الدكتورة / سحر محمد الفقي

أستاذ الأشعة التشخيصية

كلية الطب - جامعة عين شمس

الدكتورة / نهى محمد عثمان

مدرس الأشعة التشخيصية

كلية الطب - جامعة عين شمس

كلية الطب

جامعة عين شمس

٢٠١٢

# Acknowledgment

*First and foremost, I thank **Allah** the most gracious, the most merciful, for blessing this work until it reached its end as a part of his generous gifts throughout my life.*

*I wish to express my sincere thanks and deepest gratitude to **Prof. Dr. Sahar Mohamed El Feky** "Professor of Radiodiagnosis, Faculty of Medicine, Ain Shams University" for her kind supervision, constructive guidance, continuous encouragement and valuable advices she offered me to achieve this work.*

*In addition, I would like to express my profound gratitude to **Dr.Noha Mohamed Othman** "Lecturer of Radiodiagnosis, Faculty of Medicine, Ain Shams University" for her guidance suggestion, valuable comments and pieces of advice throughout the course of this essay.*

*Finally, I would like to convey my sincerest thanks to my **family, friends and colleagues** for their continuous encouragement and step-by-step help.*

*Engie El Sayed El Gohary*

## **INTRODUCTION**

Prostate cancer is the second leading cause of cancer death in men after lung cancer (*Kayhan et al., 2009*). In developing countries it may be less common, however its incidence and mortality has been on the rise (*Deongchamps et al., 2007*).

Localization of prostate cancer is important given the emergence of disease targeted therapies, such as intensity modulated radiation therapy, interstitial brachytherapy, and cryosurgery, as part of patient care. Knowledge of the tumor location within the prostate can help direct maximal therapy to the largest focus of tumor while minimizing damage to the surrounding structures, such as the neurovascular bundles, the rectal wall, and the neck of the bladder (*Haider et al., 2007*).

Routine tools for early diagnosis and localization of cancer within the prostate include digital rectal examination and assessment of serum prostate-specific antigen followed by transrectal ultrasonography guided biopsy (*Testa et al., 2007*).

Transrectal ultrasonography (US)-guided biopsy is the current reference standard for the detection of local recurrence of prostate cancer in patients with biochemical failure after external beam radiation therapy, but it is invasive and may fail to depict some tumors because only a small fraction of the gland is sampled. An accurate noninvasive alternative that enabled assessment of the entire gland would be preferable (*Westphalen et al., 2010*).

The role of CT in detection and staging of prostate cancer is limited because of poor soft tissue contrast (*Miller et al., 2010*).

MRI demonstrates zonal anatomy with excellent contrast resolution and can reveal tumours in areas not routinely sampled on biopsy and not palpable on digital rectal examination. (*Haricak, 2005*).

There is no doubt that MRI has an essential role to play in making safer, more individualized therapies possible. By revealing the anatomical location of prostate tumours, MRI can aid in staging and also provide a road-map for surgery or for radiation treatment. Moreover, the addition of proton MR spectroscopic imaging (1H MRSI) to MRI can further improve cancer localization while enhancing the assessment of tumour aggressiveness, volume and extent (*Haricak, 2005*).

To further improve the specificity and sensitivity of MR imaging, functional MR imaging techniques such as three dimensional

Hydrogen 1 MR spectroscopic imaging, dynamic contrast material enhanced MRI, and diffusion-weighted imaging have been proposed. Diffusion-weighted MR imaging is a noninvasive technique that is sensitive to the structure of biologic tissue at the microscopic level (*Mozahri et al., 2008*).

Multiparametric MRI including conventional MRI (T2), MR Spectroscopy (MRS), Dynamic contrast enhanced (DCE) and Diffusion weighted imaging (DWI) can be used to guide treatment selection particularly in high risk patients. In the future Multiparametric MRI may have a major role in selecting patients for active surveillance and/or focal therapies (*Turkbey et al., 2010*).

## **Aim of work**

The aim of this work is to spot the light on the role of MRI in detection and staging of prostate cancer.

# Contents

<b>Introduction and aim of the work</b>	<b>1</b>
<b>Anatomy of the prostate.</b>	<b>4</b>
<b>Pathology of prostate cancer</b>	<b>22</b>
<b>Technique of MRI examination of the prostate</b>	<b>33</b>
<b>A- Conventional MRI</b>	<b>33</b>
<b>B- Diffusion weighted MRI</b>	<b>41</b>
<b>C- Dynamic contrast enhanced MRI</b>	<b>48</b>
<b>D- MR spectroscopic imaging</b>	<b>60</b>
<b>Manifestations of prostatic cancer in multiparametric MRI with illustrative cases</b>	<b>71</b>
<b>A- Conventional MRI</b>	<b>71</b>
<b>B- Diffusion weighted MRI</b>	<b>77</b>
<b>C- Dynamic contrast enhanced MRI</b>	<b>85</b>
<b>D- MR spectroscopic imaging</b>	<b>97</b>
<b>Summary and conclusion</b>	<b>108</b>
<b>References</b>	<b>111</b>
<b>Arabic summary</b>	<b>-</b>

## LIST OF ABBREVIATIONS

Abbreviation	Name
<b>1.5T</b>	1.5 Tesla
<b>3D</b>	Three-dimensional
<b>3D 1H MRSI</b>	Three dimensional hydrogen proton magnetic resonance spectroscopy imaging
<b>3T</b>	3 Tesla
<b>ADC</b>	Apparent diffusion coefficient
<b>BPH</b>	Benign prostatic hyperplasia
<b>CG</b>	Central gland
<b>Cho</b>	Choline
<b>Cho + Cr / Cit</b>	Choline and creatine to citrate
<b>Cit</b>	Citrate
<b>Cr</b>	Creatine
<b>CT</b>	Computed tomography
<b>CZ</b>	Central zone
<b>DCE</b>	Dynamic contrast enhanced
<b>DHT</b>	Dihydrotestosterone
<b>DRE</b>	Digital rectal examination
<b>DTI</b>	Diffusion tensor imaging



<b>DW MRI</b>	Diffusion weighted magnetic resonance imaging
<b>DWI</b>	Diffusion weighted imaging
<b>ECE</b>	Extra capsular extension
<b>EES</b>	Extra-vascular Extra-cellular space
<b>ERC</b>	Endorectal coil
<b>FDG</b>	Fluorodeoxyglucose
<b>FOV</b>	field of view
<b>fpv</b>	Plasma volume fraction
<b>FSE</b>	Fast spin echo
<b>GH</b>	Glandular hyperplasia
<b>Hz</b>	Hertz
<b>IV</b>	Intra venous
<b>Kep</b>	Out flow kinetic constant
<b>Kg</b>	Kilogram
<b>K<sup>trans</sup></b>	Transfer constant
<b>MHz</b>	Mega hertz
<b>mm</b>	Millimeter
<b>mmol</b>	Millimol
<b>MR</b>	Magnetic resonance
<b>MRI</b>	Magnetic resonance imaging

<b>MRS</b>	Magnetic resonance spectroscopy
<b>MRSI</b>	Magnetic resonance spectroscopy imaging
<b>mSec</b>	Millisecond
<b>ng</b>	Nano gram
<b>NVB</b>	Neurovascular bundle
<b>PA</b>	Polyalanine
<b>PC</b>	Prostate cancer
<b>PET</b>	Positron emission tomography
<b>PET/CT</b>	Positron emission tomography / computed tomography
<b>PFC</b>	Perfluorcarbon
<b>PIN</b>	Prostatic intraepithelial neoplasia
<b>ppm</b>	Peak per minute
<b>PRESS</b>	Point-resolved spectroscopy
<b>PSA</b>	Prostatic specific antigen
<b>PZ</b>	Peripheral zone
<b>RF</b>	Radiofrequency
<b>ROI</b>	Region of interest
<b>s or sec</b>	Second
<b>SH</b>	Stromal hyperplasia
<b>SV</b>	Seminal vesicles

<b>SVI</b>	Seminal vesicle invasion
<b>T1 WI</b>	T1 weight image
<b>T2 WI</b>	T2 weight image
<b>tCho</b>	Total choline
<b>TE</b>	Echo time
<b>TKCM</b>	Tracer kinetic compartmental model
<b>TNM</b>	Tumor, Nodes, Metastasis
<b>TR</b>	Repetition time
<b>TRUS</b>	Trans rectal ultrasound
<b>TTP</b>	Time to peak
<b>TURP</b>	Transurethral radical prostatectomy
<b>TZ</b>	Transition zone
<b>US</b>	Ultrasonography
<b>Ve</b>	Leakage space

**B- DIFFUSION WEIGHTED MR PROSTATIC IMAGING:*****i. Principle of DW MR Examination:***

DWI is based on the molecular mobility of water (Brownian motion) (Zech et al., 2008), which is completely random in a totally unrestricted environment (Koh and Collins, 2007). The diffusion properties of tissue are related to the amount of interstitial free water and permeability (Choi et al., 2007).

This concept is supported by the fact that the mean diameter of human cells is approximately 10  $\mu\text{m}$  and the calculated root mean square displacement of water molecules during diffusion weighted imaging is reported to be 8  $\mu\text{m}$  (Pagani et al., 2008).

DWI is sensitive to changes in the microdiffusion of water within the intracellular space and extracellular space and cytotoxic edema due to alterations in the adenosine triphosphate dependent sodium (Na)-potassium (K) pumps (Bonekamp et al., 2011). The success of lesion detection and characterization largely depends on the extent of tissue cellularity because increased cellularity is associated with impeded diffusion, as indicated by a reduction in the apparent diffusion coefficient (Qayyum, 2009).

DWI sequences are usually applied in conjunction with apparent diffusion coefficient (ADC) mapping techniques. For the calculation of ADC maps, two sets of images are required: one set obtained without application of a diffusion gradient, and one obtained with a diffusion gradient. The ADC calculation is based on the negative logarithm of the ratio of those two image sets (Bitar et al., 2006).

Since the ADC values are scaled to the negative logarithm of the signal intensity ratio, areas of restricted diffusion appear dark on

ADC maps, and areas of unrestricted diffusion appear bright (**Bitar et al., 2006**).

***ii. Technique of DW in prostate imaging:***

The orientation and location of DW images are prescribed identically to the transverse T2W prostate images (**Lim et al., 2009**).

DWI is obtained with the imaging plane perpendicular to the rectal wall–prostate interface and is performed with a 1.5-T MR imaging system by using a four channel phased array surface coil coupled to an endorectal coil (**Langer et al., 2010**).

***iii. MR Diffusion Imaging data Processing:***

The ADC is calculated for each pixel of the image and is displayed as a parametric map (**Mazaheri et al., 2011**), and essentially reflects differences in tissue diffusivity at different b values. ADC measurements are then recorded for a given region by drawing regions of interest on the ADC map. Calculation of ADC is independent of magnetic field strength and the analysis is an automated process that is available as an application on most scanners or on a workstation (**Qayyum, 2009**).

***iv. MR Diffusion Imaging data Interpretation:***

DWI of PC is predicated on differences in water motion in normal versus malignant tissue (**Richstone and Ben-Levi, 2010**).

The normal prostate has an extensive branching configuration that allows water to move quite freely, whereas tumors have high cellularity and lack interstitial spaces, resulting in more restricted

diffusion (Miller et al., 2010). This is because the luminal space in benign prostate tissue is on average hundreds of microns wide, while the restrictions to water diffusion in PC is up to ten microns, a displacement scale at which DWI is sensitive (Tan et al., 2011).

As increases in cellular density affect both water diffusion and macromolecular content, therefore similarities in the statistical conclusions from ADC and T2 measurements are expected which makes correlation between ADC and T2 in the prostate is reasonable (Fig.18) (Langer et al., 2008).

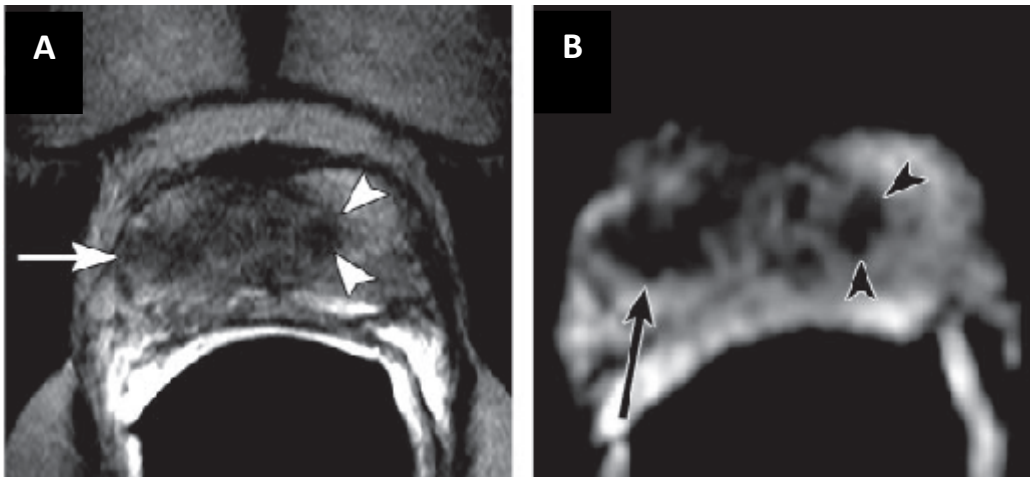


**Fig.18:** Imaging data in 68 years old man with PC. (a) Axial T2WI and (b) ADC map at the same level as (a). Two lesions with low signal intensity in PZ of right lobe (arrow) and in TZ of left lobe (arrowheads) are noted and are considered PC (Quoted from Lim et al., 2009).

The normal CZ has a lower ADC value than the PZ, on the other hand PC shows lower ADC values than the PZ, the TZ, and the CZ (Mazaheri et al., 2011), about 20%–40% lower than benign or normal prostatic tissue (Bonekamp et al., 2011).

ADC values in the Central gland increase with age, in association with the development of BPH, therefore, diagnosis of

prostate cancer with ADC measurements, especially in the CG, may be less sensitive in younger patients (**Bonekamp et al., 2011**).

**v. *Advantages of DWI of Prostate:***

1. DWI has short acquisition time and high contrast resolution between tumors and normal tissues (**Bonekamp et al., 2011**).
2. The addition of an ADC map to T2WI can improve the diagnostic performance of MRI in PC detection (**Lim et al., 2009**). The addition of DWI to T2WI increased both sensitivity and positive predictive value in the localizing PC and this improves radiation therapy planning (**Kajihara et al., 2009**).
3. DWI and calculation of ADC can potentially improve the detection of CG carcinoma (**Oto et al., 2010**).
4. The combined use of DWI and ADC value with T2WI is superior to T2WI alone for detecting seminal vesicle invasion and increases the sensitivity and specificity of urinary bladder invasion (**Tan et al., 2011**).
5. DWI and ADC value are slightly more sensitive than T2WI alone in detecting tumor within areas of hemorrhage following trans-rectal ultrasound biopsy guided (TRUS) biopsy (**Tan et al., 2011**).